NASA Contractor Report 3314

Combined Linear Theory/Impact Theory for Analysis and Design of High Speed Configurations

D. Brooke and D. V. Vondrasek

CONTRACT NAS1-15535
SEPTEMBER 1980

NASA

NASA Contractor Report 3314

Combined Linear Theory/Impact Theory for Analysis and Design of High Speed Configurations

D. Brooke and D. V. Vondrasek
McDonnell Douglas Corporation
St. Louis, Missouri

Prepared for
Langley Research Center
under Contract NAS1-15535

National Aeronautics
and Space Administration

**Scientific and Technical
Information Branch**

1980

TABLE OF CONTENTS

LIST OF ILLUSTRATIONS

SUMMARY

The application of a combined linear theory/impact theory method to calculate pressures and loadings on a wing-body configuration at Mach 4.63 was assessed. The results, compared with experimental pressure data, show that the combined method gives significantly improved predictions over either the linear theory or the impact theory method alone. The combined method was also applied in the inverse design mode at Mach 4.63 to calculate optimum camber distributions on a wing-alone, and on a wing-body configuration. The results of these optimization calculations are compared to results obtained using unmodified linear theory, and show that there is a large difference in the predicted camber distributions. Assessment of the analysis results indicates that, for the high Mach number, the optimum camber slopes obtained using the combined method are more correct than the linear theory results, and that finite thickness wings "optimized" at high Mach numbers using unmodified linear theory will not achieve the minimum drag characteristics for which they are designed.

INTRODUCTION

The feasibility of combining elements of linear theory and impact theory for improved aerodynamic predictions in the Mach 4 to 8 range was verified in Reference 1 for several wing-alone configurations. The approach is to use the aero influence coefficients (AIC) from the linear theory computer program of Reference 2 to modify the impact pressures computed in the impact theory analysis program of Reference 3. The approach provides a method of accounting for the interference effects missing from the impact theory analysis, while retaining the thickness and non-linear lifting effects characteristic of the high Mach number range.

The basic equation for the combined theory, given in matrix form, is

$$\{C_p\} = [a^{-1}] \{ \frac{\beta}{4} C_p^* \} \quad (1)$$

where $\{C_p\}$ is the column matrix of upper or lower surface pressure coefficients, $[a^{-1}]$ is the square matrix of aero influence coefficients, $\beta = \sqrt{M^2-1}$ where M is the freestream Mach number, and C_p^* represents the upper or lower surface pressure coefficients calculated using impact theory. The approach requires a one-to-one correspondence between the linear theory chord plane panels used to generate the AIC matrix and the surface elements used to represent the configuration for the impact theory calculation, i.e., the projection of the surface elements onto the chord plane must match the linear theory panels. As noted in Reference 1, the impact pressure options consistent with this analysis are tangent wedge, and Prandtl-Meyer.

The combined theory was applied to several wing-alone configurations in Reference 1, with excellent results for pressures, loadings, and forces and moments. Only in the case of comparisons near the outboard leading edge of a 76 degree swept wing were there substantial differences between predicted and measured pressures. Further analysis of that problem indicates that the differences are related to the high sweep angle, and that the over-predictions encountered will not occur unless the wing sweep exceeds about 70 degrees.

In Reference 1, the basic equation (1) was used as the starting point for a derivation of closed form approximations for the lift, drag, and moment on uncambered, wing-like bodies at high Mach numbers. Comparisons made with force and moment data on several NASA all-body models, at Mach 5.37 and 7.38, show that these closed form equations correctly predict the manner in which thickness, volume, and non-linear angle of attack effects modify

the linear theory predictions. Because of these effects, unmodified linear theory applied in the inverse optimization mode will give camber slopes which correspond to incorrect lift and moment constraints. In Reference 1, the combined theory was used to rederive the optimization equations to properly account for the thickness and higher order effects on the camber distributions.

The application of the combined theory to a wing-body configuration to calculate pressures and loadings, and to calculate optimum camber distributions, is discussed in this report. The necessary modifications to allow the computer programs given in References 2 and 3 to be used for the combined theory are also discussed.

WING-BODY ANALYSIS

The wing-body configuration discussed in Reference 4, and shown in Figure 1, was analyzed at Mach 4.63 using the combined analysis. The 65 degree swept delta wing has a symmetrical double-wedge airfoil section of 6 percent thickness ratio and joins the slender axisymmetric body at 47 percent of the body length. Pressure data is given on the body and at four spanwise locations on the wing.

For a wing-body, the basic equation (1) for the combined analysis can be separated into two equations, one for the body and one for the wing. To do this, the AIC matrix (a^{-1}) is subdivided into the submatrices which represent the body-on-body panel influence (a_{BB}^{-1}), the wing-on-body influence (a_{WB}^{-1}), the body-on-wing effects (a_{BW}^{-1}), and the wing-on-wing panel effects (a_{WW}^{-1}). The basic equation then becomes

$$\left\{C_P\right\} = \begin{bmatrix} a_{BB}^{-1} & a_{WB}^{-1} \\ a_{BW}^{-1} & a_{WW}^{-1} \end{bmatrix} \left\{\frac{\beta}{4} C_P^*\right\} \qquad (1')$$

In terms of lifting pressures, the equations for the body and wing are, respectively,

$$\{\Delta C_{P_B}\} = [a_{BB}^{-1}] \left\{ \frac{\beta}{4} \Delta C_{P_B}^{*} \right\} + [a_{WB}^{-1}] \frac{\beta}{4} \Delta C_{P_W}^{*} \}$$

$$\{\Delta C_{P_W}\} = [a_{BW}^{-1}] \left\{ \frac{\beta}{4} C_{P_B}^{*} \right\} + [a_{WW}^{-1}] \frac{\beta}{4} \Delta C_{P_W}^{*} \} \qquad (2)$$

In the equation for the body pressures (ΔC_{P_B}), the first term is simply the isolated, or body alone, pressure, and the second gives the interference contribution from the wing. In the equation for wing pressures (ΔC_{P_W}), the first term is the interference contribution from the body, and the second is the wing alone solution.

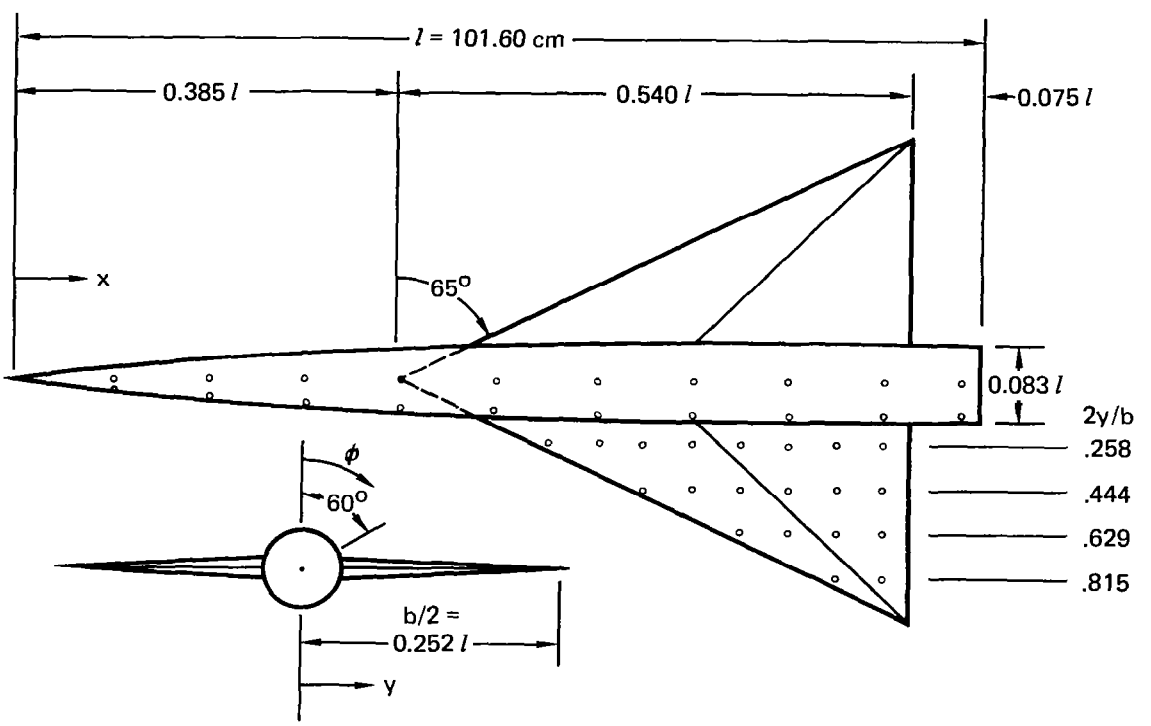

Figure 1. Sketch of Wing-Body Model from NASA TN D-6480.

Two linear theory methods were considered for the calculation of the influence coefficients. One was the program described in Reference 5, which uses surface panels on the body and chord plane panels for the wing. Although this program gave excellent predictions for the body alone pressures, a stable solution in the presence of the wing could not be achieved.

The second approach was to use an all chord plane representation (i.e., flat panels of zero thickness), as illustrated in Figure 2, and to use the program of Reference 2 to compute the influence coefficients. The pressures and loadings on the body were calculated for a variety of impact pressure options using these chord plane influence coefficients, and the results, particularly on the forebody, were poor. Figure 3 presents typical loadings on the body calculated using the chord plane influence coefficients. For comparison, the surface panel solution and the experimental pressure differences along the centerline are also shown. The large pressure peaks shown in Figure 3 are attributed to the high sweep (81 to 86 degrees) of the leading edge panels. On the afterbody, the loadings become more reasonable.

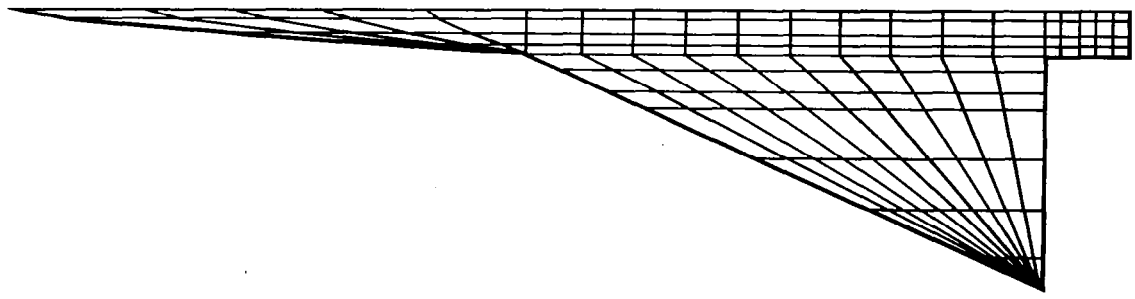

Figure 2. Chord Plane Paneling for Influence Coefficient Calculation.

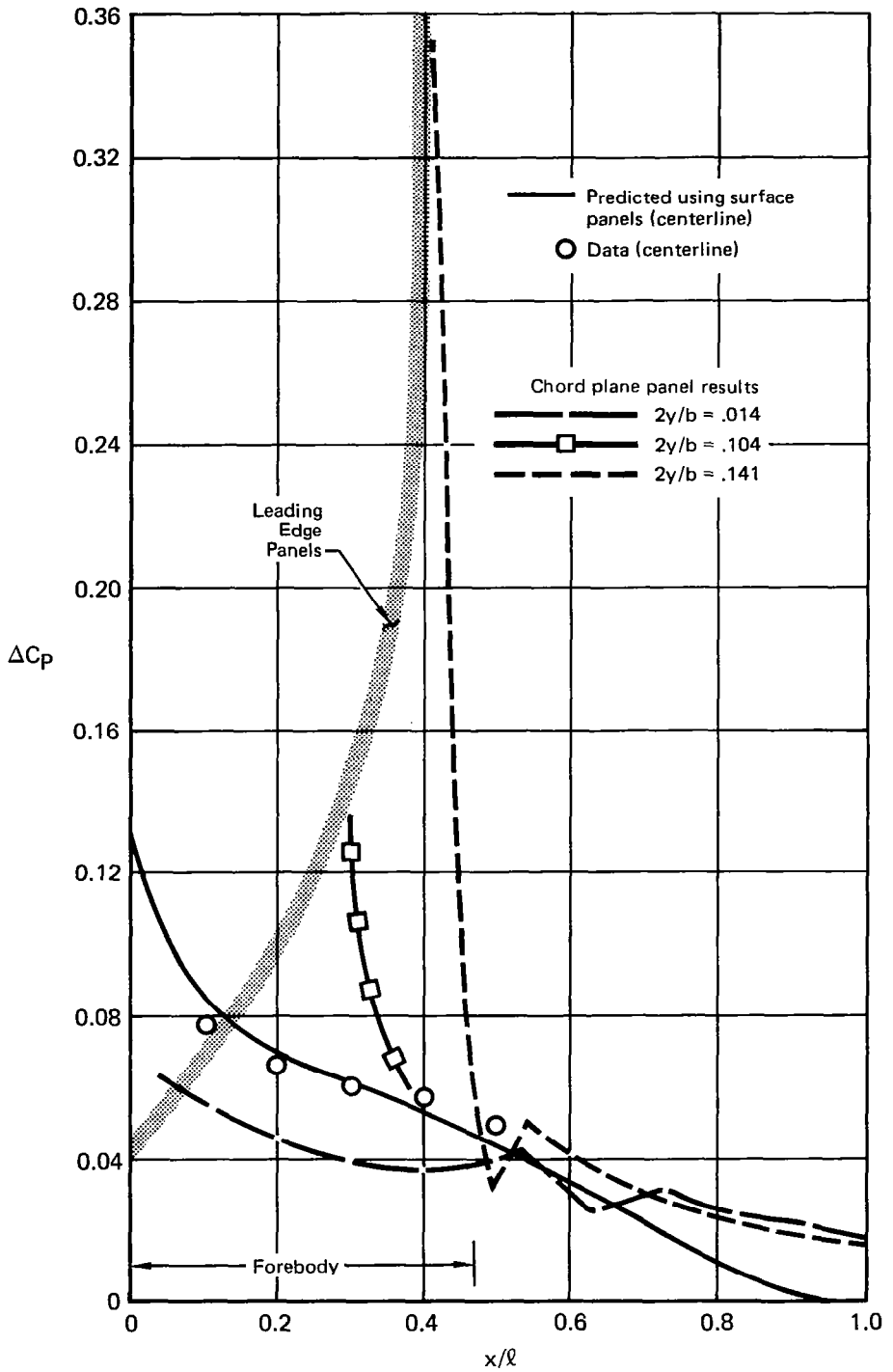

Figure 3. Predicted Loadings on Body Using Chord Plane Panels.
Mach 4.63 Angle-of-Attack = 6.2 Deg

For the body pressure calculation, it is not really necessary to use the a_{BB}^{-1} influence coefficients as computed. If the body-on-body influence coefficient matrix is replaced by a diagonal matrix, where the diagonal terms are $4/\beta$, the combined theory will give the impact theory solution on the body, plus the wing carry-over effects. If the $[a_{BB}^{-1}]$ matrix is zeroed out entirely, then only the wing interference effects are retained. These can be calculated and added to a separate isolated body solution, e.g., the surface panel method of Reference 5.

Figures 4 and 5 show the predicted pressures and loadings on the body using the latter approach. The isolated body pressures were computed using the surface panel method of Reference 5, and the wing interference pressures, calculated using tangent wedge and Prandtl-Meyer pressure options, were added directly. These results, compared with the experimental data, show that both the pressure levels and the loadings are very well predicted, both on the forebody, and in the interference region on the afterbody.

The results of the chord plane body representation shown in Figure 3 indicate that the forebody effects on the wing will be overpredicted. On the other hand, since the results on the afterbody were more reasonable, the carry-over effects from the panels aft of the wing-body junction should also be reasonable.

The pressure distributions on the wing presented in Figures 6 through 9 were computed using tangent wedge/Prandtl-Meyer (TW/PM) impact pressures on the wing and aft portion of the body. Three different pressure options were considered on the forebody. These were: (1) tangent wedge/Prandtl-Meyer, where the forebody was treated as a flat plate. This calculation gives essentially the same carry-over loadings on the wing that unmodified linear theory gives. (2) A tangent cone (TC) approximation was used, where

$$C_{P_{TC}}^{*} = \pm\, 2 \sin^{2}\delta$$

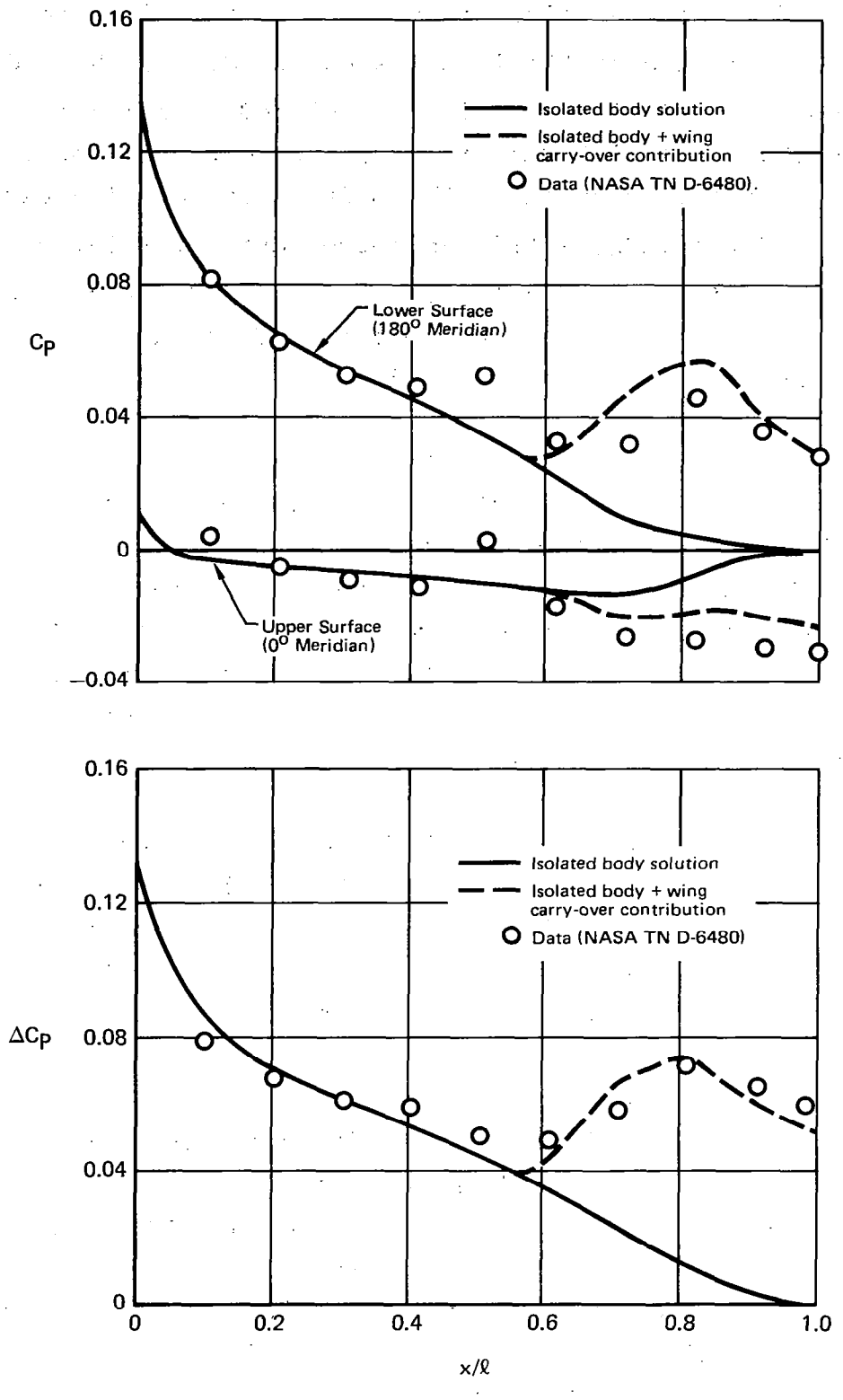

Figure 4. Pressure Distribution and Loading on Body Centerline, Mach 4.63 Angle-of-Attack = 6.2 Deg

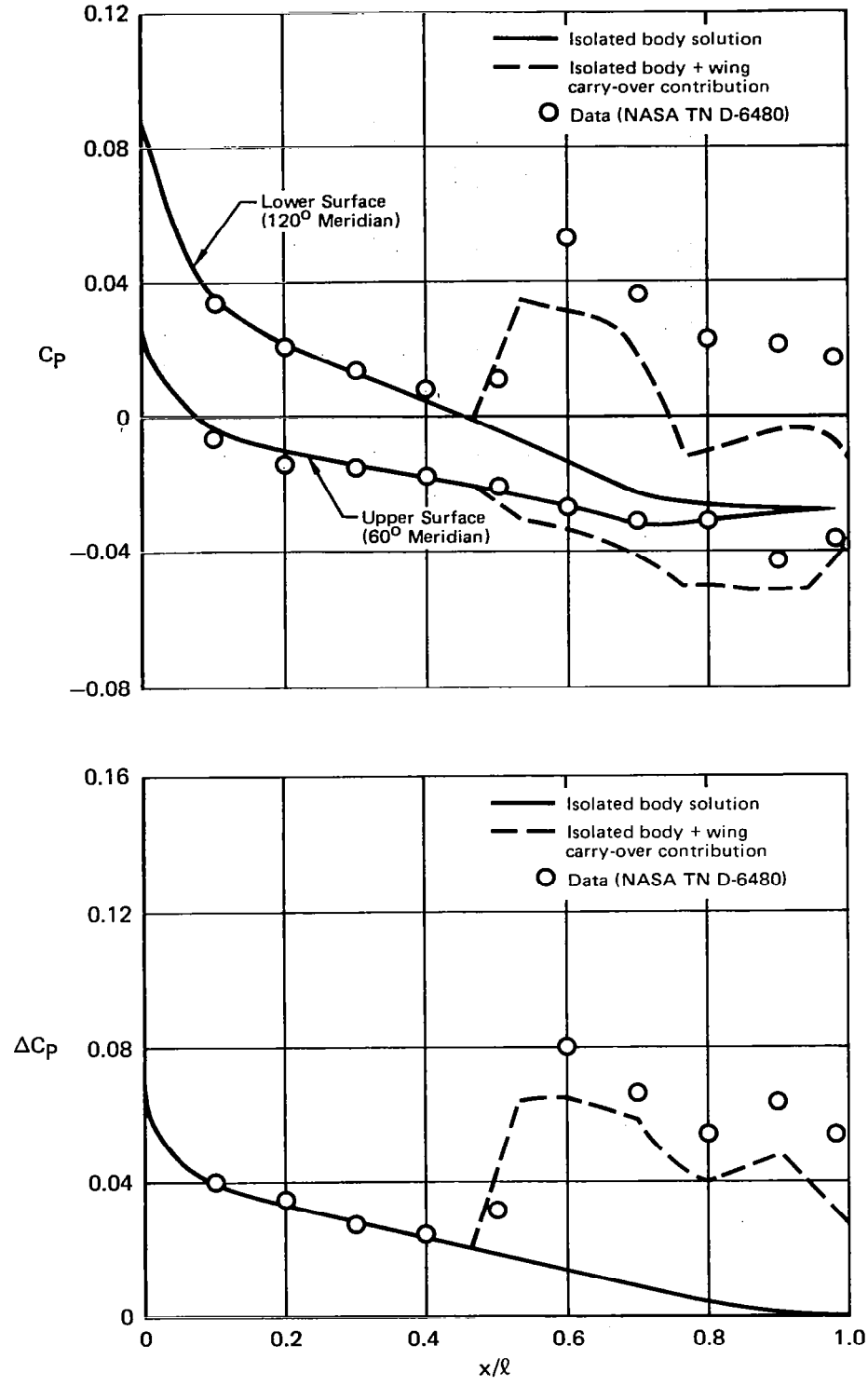

Figure 5. Pressure Distribution and Loading on Body (60 and 120 Deg Meridians), Mach 4.63 Angle-of-Attack = 6.2 Deg

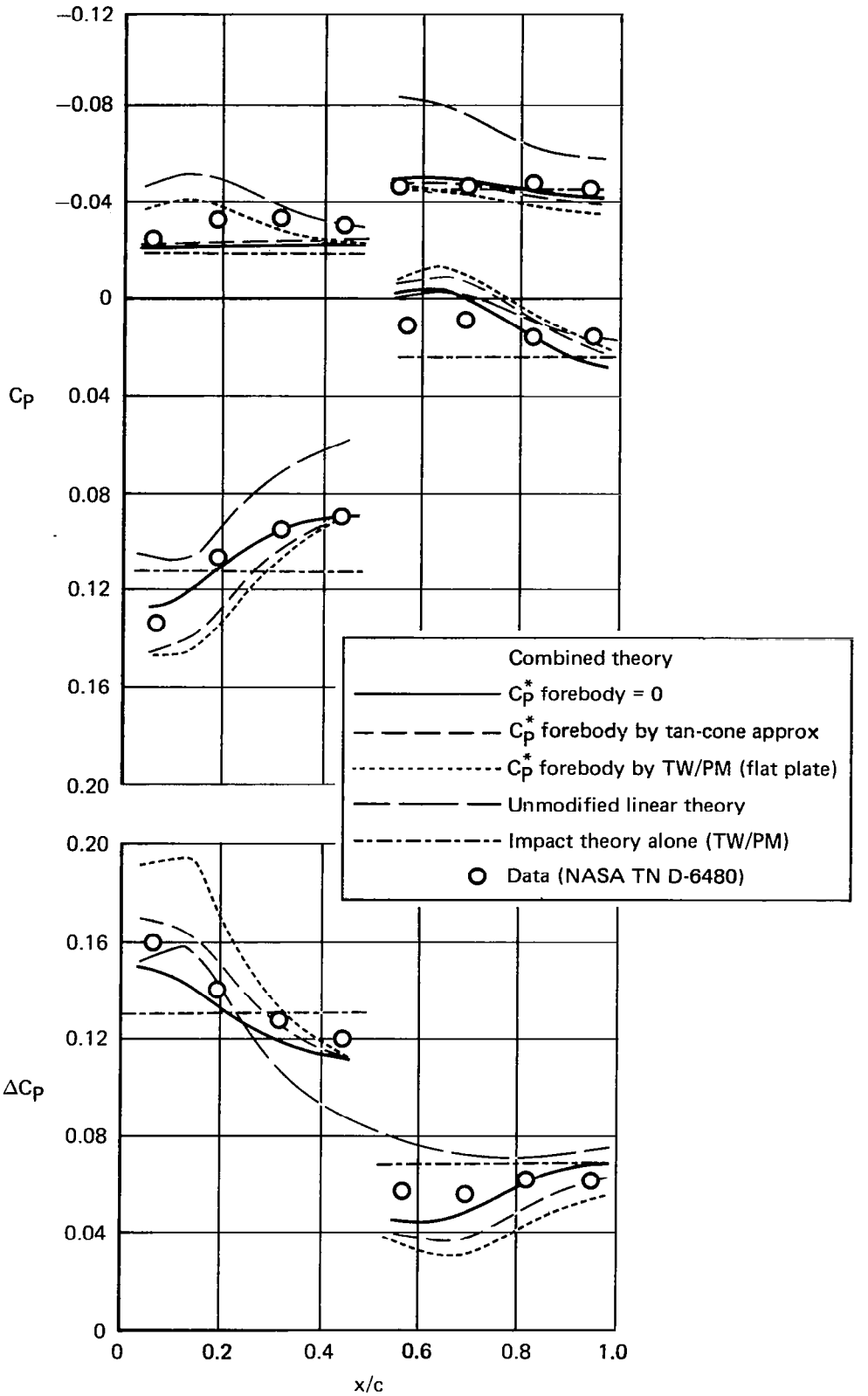

Figure 6. Wing Pressures and Loadings (y/b/2 = 0.258),
Mach 4.63 Angle-of-Attack = 6.2 Deg

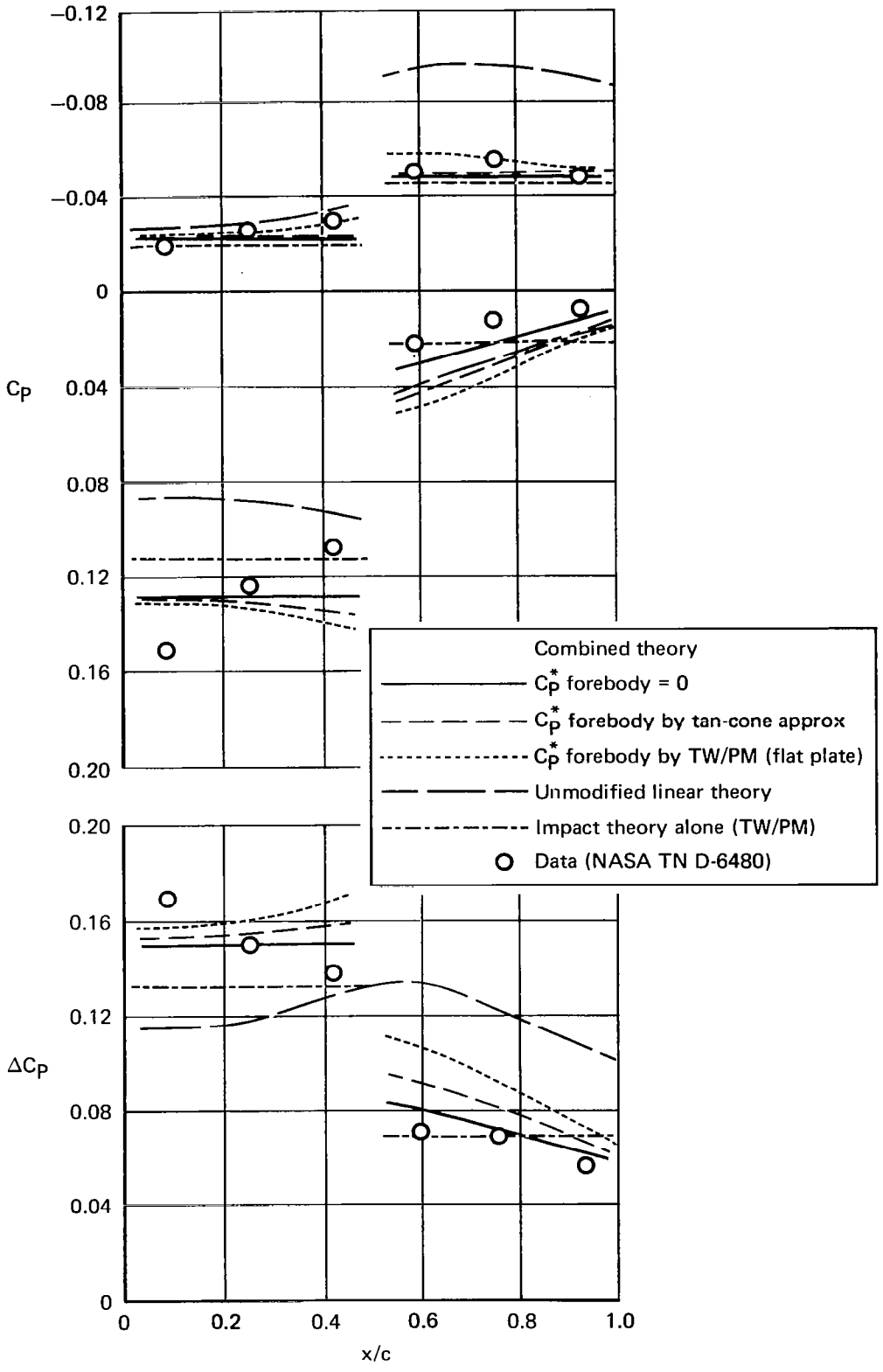

Figure 7. Wing Pressures and Loadings (y/b/2 = 0.444).
Mach 4.63 Angle-of-Attack = 6.2 deg

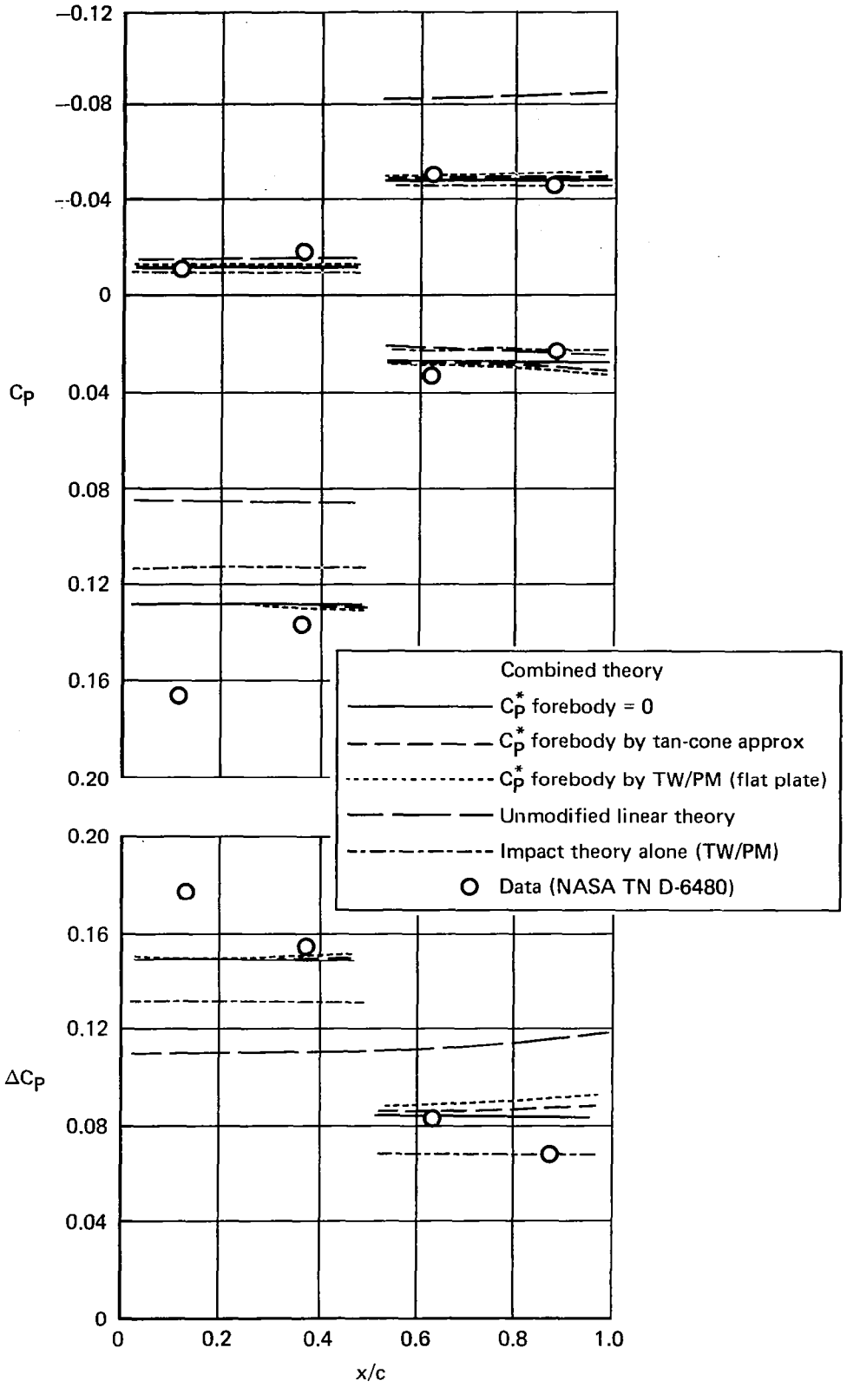

Figure 8. Wing Pressures and Loadings (y/b/2 = 0.629).
Mach 4.63. Angle-of-Attack = 6.2 deg

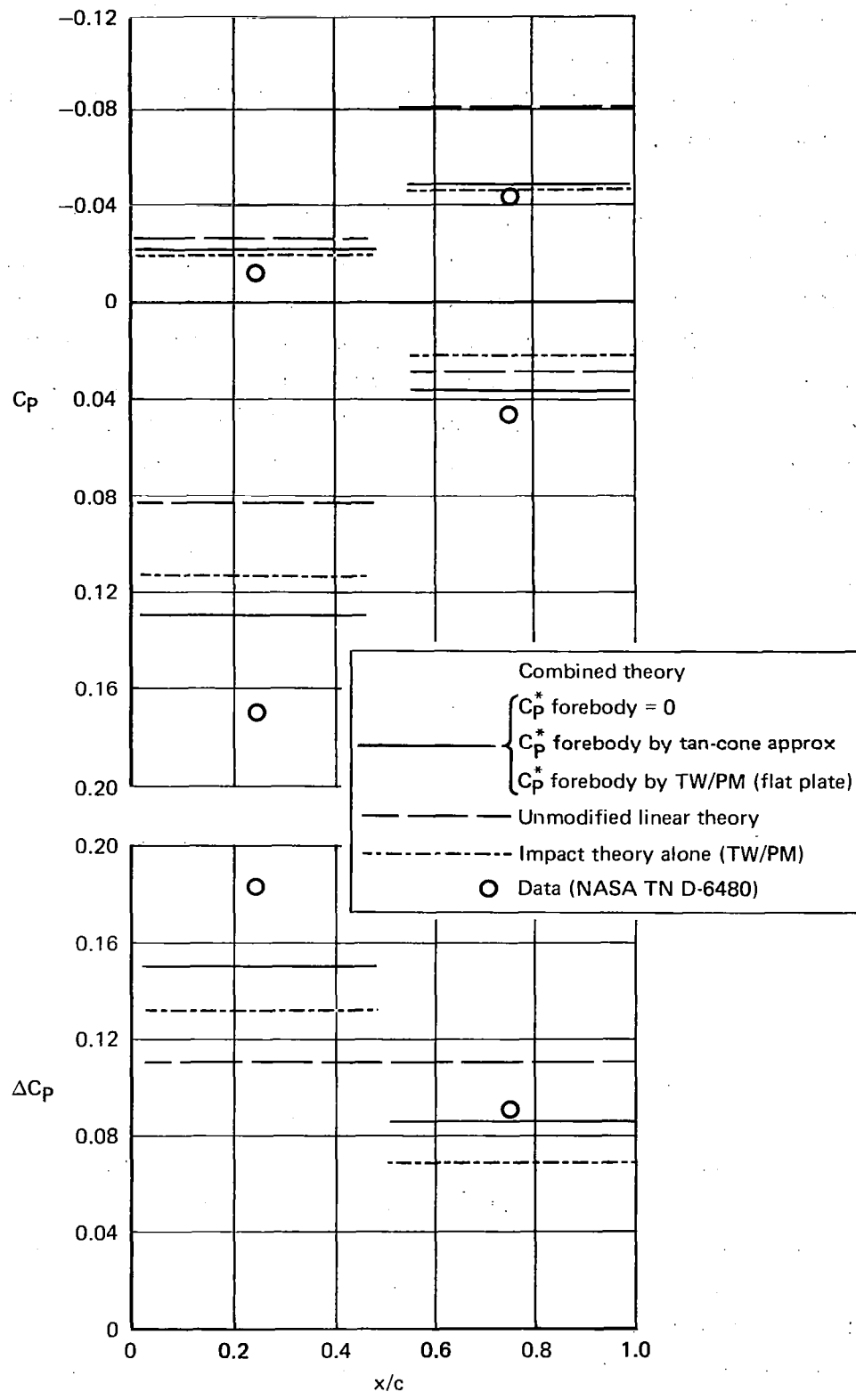

Figure 9. Wing Pressures and Loadings (y/b/2 = 0.815).
Mach 4.63 Angle-of-Attack = 6.2 deg

and δ is the local surface slope measured from the freestream. For negative values of δ, the minus sign in the above equation is used. And (3), the wing pressures were computed with the forebody pressures set to zero.

The results of the calculations for the wing pressures are compared with the measured data in Figures 6 through 9. Results from unmodified linear theory on a chord plane representation of the wing are also shown, along with a standard impact theory (TW/PM) solution for the wing surface panels. The comparisons at all four wing stations show that the combined theory gives better predictions for both pressures and loadings than either linear theory, or impact theory. For the combined theory results, the best predictions were obtained for the forebody pressures set to zero, suggesting that the slender forebody actually contributes very little influence on the wing. The use of both the tangent cone approximation, and the tangent wedge/Prandtl-Meyer calculation, led to overpredictions at the inboard wing stations. These overpredictions occur along the Mach line emanating from the highest pressure peaks on the forebody (Figure 3), and reflect the difficulty in simulating the flow on a slender axisymmetric body using a chord plane representation.

OPTIMIZATION

Figures 6 through 9 show that at each spanwise location on the wing, the center of lift is much further forward than predicted by linear theory. This is because the thickness contributions to the lifting pressures, which become important at high supersonic Mach numbers, are not included in the linear theory. Depending on the thickness distributions, the linear theory will not correctly predict the lift and/or moment characteristics of finite thickness wings at high Mach numbers. Conversely, the "optimum" camber distributions calculated using unmodified linear theory will correspond to incorrect lift and moment constraints.

As discussed in Reference 1, the combined theory permits the inclusion of the thickness effects in the inverse design procedure. The optimization equations from Reference 2 were modified to include the thickness contributions to the lifting pressures, and the equations are presented in Figure 10. These equations were used to calculate the optimum camber slopes on the theoretical wing from the wing-body configuration in Figure 1. The camber slopes were calculated at Mach 4.63 for a design lift coefficient ($\bar{C}_L$) of 0.1 and a design moment coefficient ($\bar{C}_m$) of 0.0. The moment reference center was at 50 percent of the mean aerodynamic chord (.5$\bar{c}$). The calculated camber slopes using the combined theory are compared with the unmodified linear theory results in Figure 11.

The comparisons in Figure 11 show that there is a significant difference in the predicted camber distributions. The reason for the large difference is illustrated in Figure 12, which shows the lift and moment characteristics for the uncambered wing as predicted by the combined theory and linear theory. Although the lift curve slope for this wing is the same for both theories, the combined theory shows that the wing is 9.5 percent unstable, while the linear theory predicts the wing to be neutrally stable. Thus, the moment constraint ($\bar{C}_{M_{.5\bar{C}}} = 0.0$) is not a driver in the linear theory analysis, and the camber slopes do not deviate much from a 6.63 degree flat plate angle of attack needed to obtain a lift coefficient of 0.1.

On the other hand, the combined theory predicts that, at a lift coefficient of 0.1, the camber must effectively trim out a moment coefficient of 0.0095. Since the thickness effects shift the loading forward, relative to the linear theory, the forward portion of the wing must be drooped more than predicted by the linear theory to decrease the moment, and to satisfy the moment constraint. As a consequence of the greater variation in camber slopes, the minimum drag due to lift is about 5 percent higher than predicted by the linear theory alone.

OPTIMIZATION MATRIX - Solution gives loadings for minimum drag corresponding to lift and moment constraints

$$\begin{bmatrix} \left(\frac{s_1 a_{11}}{b_1} + \frac{s_1 a_{11}}{b_1}\right) & \left(\frac{s_1 a_{12}}{b_1} + \frac{s_2 a_{21}}{b_2}\right) & \left(\frac{s_1 a_{13}}{b_1} + \frac{s_3 a_{31}}{b_3}\right) \ldots s_1 & s_1(\bar{x} - x_1) \\ \left(\frac{s_2 a_{21}}{b_2} + \frac{s_1 a_{12}}{b_1}\right) & \left(\frac{s_2 a_{22}}{b_2} + \frac{s_2 a_{22}}{b_2}\right) & \left(\frac{s_2 a_{23}}{b_2} + \frac{s_3 a_{32}}{b_3}\right) \ldots s_2 & s_2(\bar{x} - x_2) \\ \left(\frac{s_3 a_{31}}{b_3} + \frac{s_1 a_{13}}{b_1}\right) & \left(\frac{s_3 a_{32}}{b_3} + \frac{s_2 a_{23}}{b_2}\right) & \left(\frac{s_3 a_{33}}{b_3} + \frac{s_3 a_{33}}{b_3}\right) \ldots s_3 & s_3(\bar{x} - x_3) \\ \ldots & & & \\ s_1 & s_2 & s_3 \ldots 0 & 0 \\ s_1(\bar{x} - x_1) & s_2(\bar{x} - x_2) & s_3(\bar{x} - x_3) \ldots 0 & 0 \end{bmatrix} \begin{bmatrix} \Delta C_{P_1} \\ \Delta C_{P_2} \\ \Delta C_{P_3} \\ \ldots \\ \Lambda_1 \\ \Lambda_2 \end{bmatrix} = \begin{bmatrix} 0 \\ 0 \\ 0 \\ \ldots \\ \bar{L} \\ \bar{M} \end{bmatrix}$$

OPTIMUM CAMBER - Calculated from optimum loadings

$$\alpha_i = \frac{1}{b_i} \sum_j a_{ij} (\Delta C_{p_j})_{OPT}$$

where s_i = area of element i

a_{ij} = influence coefficient (element i on element j)

b_i = $1 + 1.2\beta \epsilon_i + 0.6\beta^{3/2} \epsilon_i^2$ (thickness factor from Ref. 3 Program) and ϵ_i is thickness slope

ΔC_{p_i} = pressure difference on element i

$\bar{x} - x_i$ = distance from moment ref to centroid of element i

Λ_1, Λ_2 = Langrangian multipliers

$\bar{L}, \bar{M}$ = design lift and moment constraints

$\bar{L} = \bar{C}_L qS \quad \bar{M} = \bar{C}_M qS\bar{c}$

Figure 10. Optimization Matrix for Design Procedure.

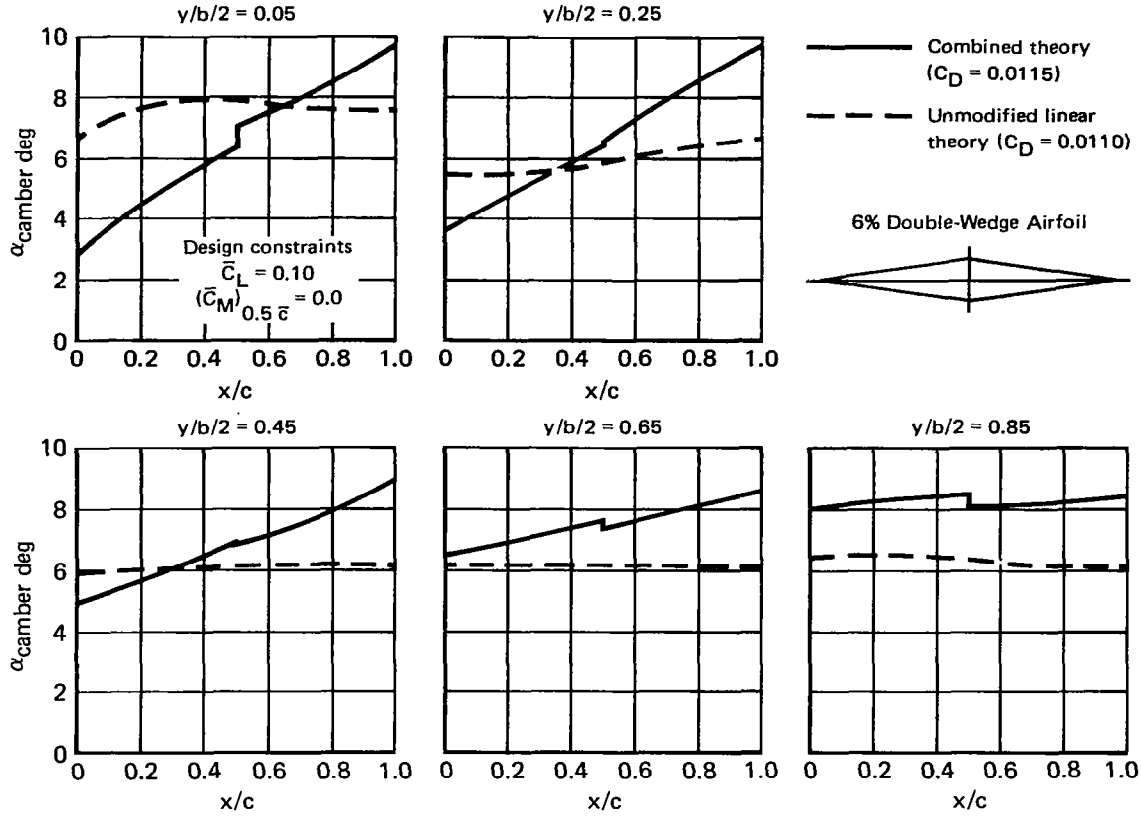

Figure 11. Predicted Camber Distributions for Minimum Drag
65° Swept Delta Wing @ Mach 4.63

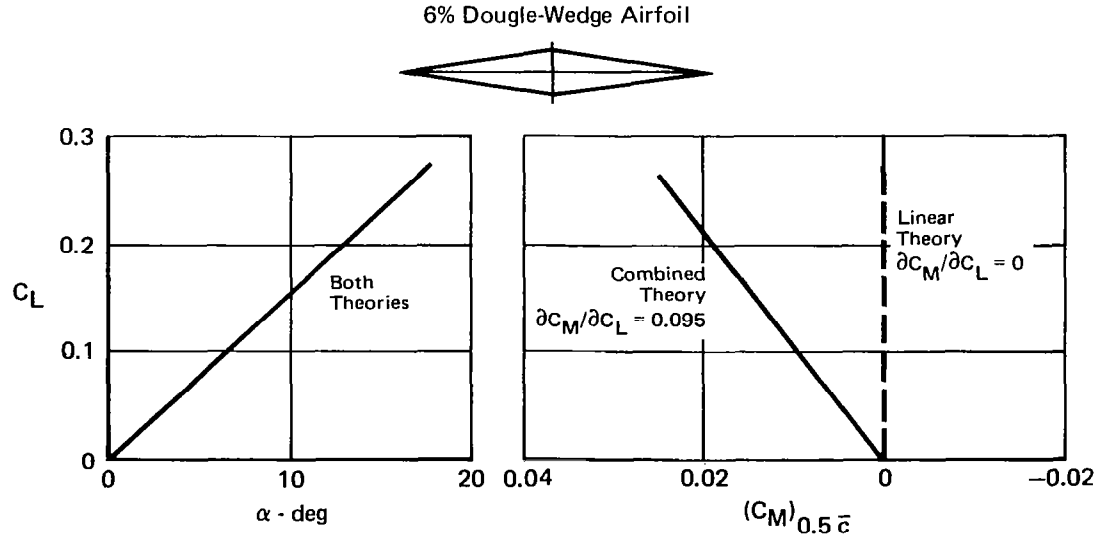

Figure 12. Lift and Moment Characteristics of Uncambered Wing
65° Swept Delta Wing at Mach 4.63

The minimum drag characteristics for the wing-body (Figure 1), for the same lift and moment constraints used above, are illustrated in Figure 13 as a function of the moment reference location (X_{CG}). For these calculations, the panels representing the body were constrained at 6.2 degrees angle of attack. Without the camber constraint on the body, the solution tends to give unrealistically large camber slopes on the forebody.

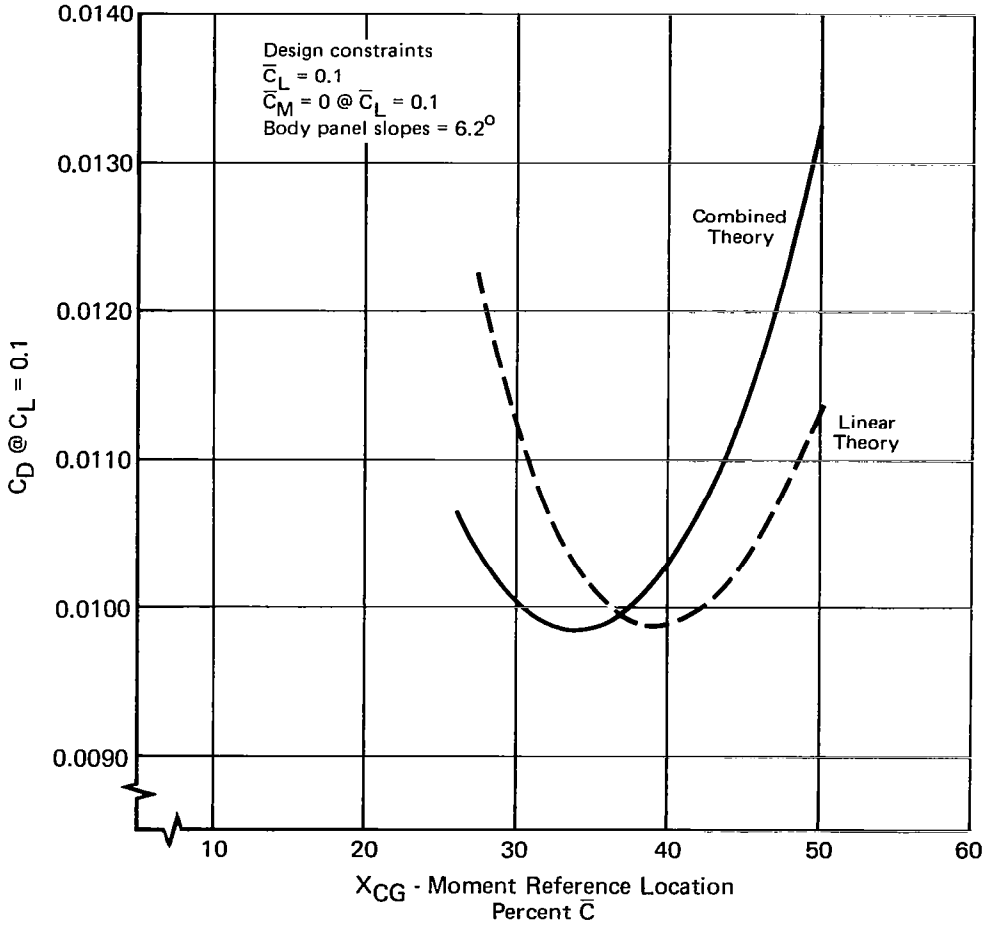

Figure 13. Minimum Drag Due to Lift as Function of Moment Reference Location.
Wing-Body Configuration @ Mach 4.63

Assuming the combined theory results reflect the true situation (a reasonable assumption in view of the results shown in Figures 6 through 9), the minimum drag is achieved for the center of gravity at 34 percent of the mean aerodynamic chord. For this moment reference location, the linear theory slopes give higher drag. Since the neutral point is incorrectly predicted, the linear theory camber slopes will also fail to meet the moment constraint. Because of this, trimming devices would have to be used, resulting in even higher drag.

COMPUTER PROGRAMS

The computer programs described in References 2 and 3 were used to perform the combined linear theory/impact theory calculations described in this report and in Reference 1. Although various versions of the Reference 2 program may be in use, so long as the essential subroutines (EVAL, INVW, MDMATE, FCALC, CAMBW and DCPD) are contained in those programs, they may be used for the linear theory portions of the combined calculation. For these calculations, only minor modifications to subroutines INVW, MDMATE, CAMBW, and DCPD are required. It should be noted that only INVW need be modified to obtain the inverted AIC matrix for use in the impact theory analysis. For optimum camber calculations, MDMATE, CAMBW, and DCPD need to be modified. The actual modifications to these routines are given in Appendix A.

The impact theory program (Reference 3) is used to calculate the impact pressures, and, using the AIC matrix, to calculate the combined theory pressures. To perform the pressure calculation, a new subroutine (CPCALC) is added to the program, along with minor changes to subroutines PRES and FORCE which provide required control information. The thickness factors needed in the optimization matrix are calculated in CPCALC. The modifications to the program are given in Appendix B.

RESULTS AND CONCLUSIONS

The results of this study demonstrate that the combined linear theory/impact theory provides an accurate, versatile, and easy to use method for the analysis and design of configurations at high Mach numbers. The combination of the supersonic linear theory and the hypersonic impact theory overcomes many of the problems encountered by the individual theories when used in the Mach 4 to 8 range. In addition, only the simplest combination of characteristics from the linear and impact approaches are required to produce consistently good results. Oblique shock theory (or Newtonian) and Prandtl-Meyer expansion coupled with a chord plane representation of the geometry to generate the aerodynamic influence coefficient matrix is considered the basic calculation method. However, by partitioning the aerodynamic influence coefficient matrix, the basic approach becomes flexible enough to permit a multitude of combinations which may become more evident through continued applications and comparisons with experiment.

The results of the wing-body comparisons show that the combined theory gives improved analysis results over either the linear theory or the impact theory methods alone. The application of the combined theory in the inverse design mode shows that the use of unmodified linear theory to calculate optimum camber slopes will lead to incorrect results at high supersonic Mach numbers. The combined theory offers the prospect of improved high speed designs by providing a more appropriate optimization procedure. Only minor modifications to existing state-of-the-art computer programs are needed to implement the combined theory, and these modifications will not affect the normal, stand-alone operation of the programs, nor require changes in existing input data decks.

APPENDIX A
LINEAR THEORY PROGRAM MODIFICATIONS

The modifications to the linear theory program documented in NASA CR-73107 (Part II) are given below. The listings of the subroutines affected have been extracted from the NASA documentation and the appropriate changes are noted.

In the analysis mode, the program is used to generate the AIC matrix and to write the matrix onto a tape, which can be accessed by the impact theory program. It is assumed that the user will specify an appropriate output device and the necessary job control cards to save the output tape. Further, it is assumed that the AIC matrix will be calculated using the "wing alone" or all chord plane paneling option. The AIC matrix is obtained from subroutine INVW, as shown in Figure A-1. Note that this is the inverted matrix, $[a^{-1}]$.

For the inverse design or optimum camber calculations, the MDMATE and CAMBW routines are modified to read in and to use the thickness factor terms from the impact theory program. Again, it is assumed that the user will supply the appropriate tape number and job control cards to allow the program to access the output tape from the impact theory program. Subroutine DCPD should also be modified in case the configuration is run through a series of angle of attacks using the calculated camber slopes. The modification in DCPD corrects the loading distributions (ΔC_p's) consistent with the combined theory and gives the corrected lift and moment characteristics. The calculated camber distributions, and the corresponding loadings are printed in the normal output (pages 102-104 in Part II) under the headings "WING CAMBER SLOPES (DZ/DX)" and "WING PANEL PRESSURE DIFFERENCE (CL)," respectively. Note that with the exception of the input of an indicator to tell the program to read a tape, all other inputs are unchanged. If the indicator is placed in an unused field on one of the standard

```
      SUBROUTINE INVW

C     FOR WING ONLY CASE, STORES MATRIX (A) AND (A) INVERSE ON TAPE
C     MAXIMUM SIZE MATRIX INVERSION =110


      COMMON DATE(2),NTAPEA,NTAPEB,NTAPEC,NTAPED,NTAPEE,NTAPEF,NTAPEI
     1,NTAPEO,NBODY,NWING,XMACH,SYM,KACE

      DIMENSION AWW(115,115)

      MDEMEN=115

C     READ (A) MATRIX INTO CORE, WRITE ON TAPE

      CALL FSF(1,NTAPEA,IRR)
      DO 100 J=1,NWING
      READ (NTAPEA) (AWW(I,J),I=1,NWING)
      WRITE (NTAPEE) (AWW(I,J),I=1,NWING)
  100 CONTINUE
      END FILE NTAPEE
      REWIND NTAPEA


C     INVERT MATRIX (A)

      CALL SINVRT(AWW,MDEMEN,NWING,IRR1,IRR2,SCALE,DET,NDETXP)
      IF (IRR1) 150,200,150
  150 WRITE (NTAPEO,6000) IRR1,IRR2,SCALE
      REWIND NTAPEE
      STOP


  200 CONTINUE
      DO 250 J=1,NWING
      WRITE (NTAPEE) (AWW(I,J),I=1,NWING)
  250 CONTINUE
      END FILE NTAPEE
      REWIND NTAPEE


 6000 FORMAT(1H1,38HERROR IN INVERSION OF WING ONLY MATRIX
     1,5X,6HIRR1 =,I3,5X,6HIRR2 =,I3,5X,7HSCALE =,E12.6)

      RETURN
      END
```

FROM PAGE 671 OF REF. 2 - PART II

(A) →

(A)

```
      NTAPES= *
      WRITE(NTAPES) (AWW(J,I), I=1,NWING)
```

* REQUIRES DEFINITION OF NTAPES

Figure A-1. Modifications to Subroutine INVW.

input cards, such that it defaults to zero if not specified, then the modifications, given in Figures A-2 to A-4, will not affect the normal operation of the program.

```
      SUBROUTINE MDMATE

C     FORMATION OF DRAG MINIMIZATION MATRIX
C     MAXIMUM SIZE MATRIX INVERSION =112
C     MUST BE 2 PLUS MAXIMUM NUMBER OF WING PANELS(110)

      COMMON DATE(2),NTAPEA,NTAPEB,NTAPEC,NTAPED,NTAPEE,NTAPEF,NTAPEI
     1,NTAPEO,NBODY,NWING,XMACH,SYM,KACE
(A)-->
      DIMENSION WW(115,115),XBAR(210),AREA(210)

      MDEMEN=115
      READ (NTAPEC) NBODY,NWING,XMACH,SYM,KACE
      NPANEL=NBODY+NWING
      READ (NTAPEC) (I,XBAR(I),DUMMY1,DUMMY2,DUMMY3,DUMMY4,DUMMY5
     1,AREA(I),DUMMY6,DUMMY7,DUMMY8,I=1,NPANEL)
      REWIND NTAPEC

      DO 100 J=1,NWING
      READ (NTAPEE) (WW(I,J),I=1,NWING)
  100 CONTINUE
      REWIND NTAPEE                                  FROM PAGE 686 OF
(B)-->                                               REF. 2 - PART II
      DO 200 I=1,NWING
      I=I
      II=I+NBODY
      DO 200 J=1,I
      JJ=J+NBODY
      WW(I,J)=-WW(I,J)*AREA(II)-WW(J,I)*AREA(JJ)
      WW(J,I)=WW(I,J)
  200 CONTINUE
```

(A)

```
      COMMON /BFACT/BMD(110)
```

(B)

```
      DO 50 J=1,NWING
   50 BMD(J)=1.0
      READ(5,99) BIND
   99 FORMAT(F10.1)
      IF (BIND.EQ.0.0) GO TO 170
      NTAPET= *
      READ(NTAPET) (BMD(I),I=1,NWING)
      DO 150 J=1,NWING
      DO 150 I=1,NWING
  150 WW(I,J)=WW(I,J)/BMD(I)
  170 CONTINUE
```

* REQUIRES DEFINITION OF NTAPET

Figure A-2. Modifications to Subroutine MDMATE.

```
      SUBROUTINE CAMBW (NW,NTAPEX,A,CLW,ALPHAW)
      DIMENSION A(1),ALPHAW(1),CLW(1)
C     FOR WING ONLY CASE, COMPUTES NORMAL VELOCITY COMPONENTS ON WING
      DO 100 J=1,NW
      ALPHAW(J)=0.0
  100 CONTINUE
      DO 200 J=1,NW
      READ (NTAPEX) (A(I),I=1,NW)
      DO 200 I=1,NW
      ALPHAW(I)=ALPHAW(I)+A(I)*CLW(J)
  200 CONTINUE
      RETURN
      END
```

FROM PAGE 506 OF REF. 2 - PART II

```
      COMMON /BFACT/BMD(110)
      DO 300 I=1,NW
      ALPHAW(I)=ALPHAW(I)/BMD(I)
  300 CONTINUE
```

Figure A-3. Modifications to Subroutine CAMBW.

```
      SUBROUTINE DCPD(NM,NTAPEX,A,ALPHAM,CLM)
C     COMPUTES WING PANEL PRESSURE DIFFERENCE
      DIMENSION A(1),ALPHAM(1),CLM(1)
      DO 100 J=1,NM
      CLM(J)=0.0
  100 CONTINUE
      DO 200 J=1,NM
      READ (NTAPEX) (A(I),I=1,NM)
      DO 200 I=1,NM
      CLM(I)=CLM(I)+A(I)*ALPHAM(J)
  200 CONTINUE
      RETURN
      END
```

FROM PAGE 535 OF REF. 2 - PART II

```
      COMMON /BFACT/BMD(110)
      CLM(I)=CLM(I)+A(I)*ALPHAM(J)*BMD(J)
```

Figure A-4. Modifications to Subroutine DCPD.

APPENDIX B
IMPACT THEORY PROGRAM MODIFICATION

The modifications to the impact theory program documented in AFFDL-TR-73-159 (VOl. III) are discussed below. Two subroutines (PRES and FORCE) are modified, and a new subroutine (CPCALC) has been added.

In the PRES routine, two control parameters (IWOOD and IROW) are read in and placed in common. The required changes are given in Figure B-1. The card identification numbers correspond to the ID numbers in the reference listing. The modifications to the FORCE subroutine are given in Figure B-2, and the subroutine CPCALC is listed in Figure B-3.

The parameters IWOOD and IROW control the calculation of the indices of the influence coefficients corresponding to the impact theory panels. IROW is the number of panels, leading edge to trailing edge, in the linear theory representation. Three options are provided for IWOOD. These are:

IWOOD = 0 The normal operation of the program is unaffected.

IWOOD = 1 The AIC matrix will be read-in and the combined theory pressures, and forces and moments will be calculated. The strip input option is used to define the geometry. The upper surface panels are input in the same order as the linear theory panels. The lower surface panels are then input in reverse order, i.e., the last panel on the lower surface corresponds to the first panel of the upper surface.

```
REPLACE PRES 8 WITH
     COMMON /GDATA/LTOT,J,SYMFCT,IORN,IGTYPE,L,IWOOD,IROW

REPLACE PRES 53 WITH
     READ(TAPEIN,20) NCOMP,IFSAVE,TITLE,IWOOD,IROW

REPLACE PRES 54 WITH
 20  FORMAT(I2,I1,3X,15A4,2I2)
```

Figure B-1. Modifications to PRES Subroutine.

```
REPLACE FORC 12 WITH
     COMMON /GDATA/LTOT,J,SYMFCT,IORN,IGTYPE,L,IWOOD,IROW


INSERT BETWEEN FORC 23 AND FORC 24
     COMMON /CPARRY/ICPS,LTS,CPS(224),BETAM,DELT(224)

INSERT BETWEEN FORC 35 AND FORC 36
     BETAM=SQRT(MACH**2-1.)
     ICPS=-1
 1   ICPS=ICPS+1

INSERT BETWEEN FORC 223 AND FORC 224
     DELT(L)=DELTAR

INSERT BETWEEN FORC 571 AND FORC 572
     IF (ICPS.EQ.0)  CPS(L)=CP
     IF (ICPS.EQ.1)  CP=CPS(L)

INSERT BETWEEN FORC 749 AND FORC 750
     IF ((ICPS.EQ.0).AND.(IWOOD.NE.0))  CALL CPCALC
     IF (ICPS.EQ.1)  GO TO 1
```

Figure B-2. Modifications to Subroutine FORCE (Next, IG4S).

```
      SUBROUTINE CPCALC
C***************
C     THIS ROUTINE USES THE INVERTED MATRIX (A) FROM WOODWARD
C      TO ADJUST THE COMPONENT CP VALUES CALCULATED IN FORCE SUBR.
C***************
      COMMON /GDATA/LTOT,JJ,SYMFCT,IURN,IGTYPE,LL,IWOOD,NROW
      COMMON /CPARRY/ ICPS,LTS,CPS(224),BETAM,FACT,DELT(224)
      COMMON /TAPE/ TAPEIN,TAPEOT
      DIMENSION CP(224),A(110,110),[redacted],B(110)

      INTEGER TAPEIN,TAPEOT
C
CC    READ (A) ARRAY
C
      NTAPE=15
      REWIND15
      LT=2*(LTS/2)
      L=LT/2
      L1=L+1
      DO 10 I=1,L
      READ (NTAPE,200) (A(I,J),J=1,L)
   10 CONTINUE
C
CC    CALCULATE THICKNESS FACTOR
C
      DO 15 J=L1,LT
      M=NROW+2*NROW*((J-L1)/NROW)-(J-L1)
      IF(IWOOD.EQ.2)M=J-NROW-2*NROW*((J-L1)/NROW)
      ETA=(DELT(M)+DELT(J))/2.
      ALPH=(DELT(J)-DELT(M))/2.
   15 B(M)=1.+1.2*BETAM*ETA+.6*BETAM**1.5*ETA**2
C
CC    CALCULATE UPPER SURFACE
C
      DO 20 I=1,L
      CP(I)=0.
      DO 20 J=1,L
      CP(I)=CP(I) + A(I,J)*CPS(J)
   20 CONTINUE
C
CC    CALCULATE LOWER SURFACE
C

      DO 30 I=L1,LT
      CP(I)=0.
      K=NROW+2*NROW*((I-L1)/NROW)+1-(I-L)
      IF(IWOOD.EQ.2)K=I-NROW-2*NROW*((I-L1)/NROW)
      DO 25 J=L1,LT
      M=NROW+2*NROW*((J-L1)/NROW)-(J-L1)
      IF(IWOOD.EQ.2)M=J-NROW-2*NROW*((J-L1)/NROW)
      CP(I)=CP(I) + A(K,M)*CPS(J)
   25 CONTINUE
      CP(I)=CP(I)*BETAM/4.
   30 CONTINUE
C
CC       WRITE CPS ARRAY FROM FORCE SUBR.
C
      WRITE (TAPEOT,210)
      WRITE(TAPEOT,200) (CPS(I),I=1,LTS)
      DO 40 I=1,LT
      CPS(I)=CP(I)
   40 CONTINUE
C
C        WRITE CP ARRAY CALCULATED HERE
      WRITE (TAPEOT,220)
      WRITE (TAPEOT,200) (CPS(I),I=1,LTS)
      ICPS=1
      WRITE(TAPEOT,230)
      WRITE(TAPEOT,200) (B(I),I=1,L)
  200 FORMAT(1X,8E15.8)
  210 FORMAT(1H1,20X,35HCOMPONENT CP VALUES FROM FORCE SUBR.//)
  220 FORMAT(1H1,20X,28HADJUSTED COMPONENT CP VALUES.//)
  230 FORMAT(1H1)
      RETURN
      END
```

Figure B-3. Subroutine CPCALC

IWOOD = 2 The combined theory calculations are performed, but the geometry is input in the NASA wave drag format.

When the combined calculations are performed, the unmodified impact pressures are computed, along with the forces and moments, and output in the normal output format. Then the combined theory pressures, and the corresponding forces and moments, are calculated and output at the same angle of attack. The output is, again, in the normal output format.

REFERENCES

1. Brooke, D.; and Vondrasek, D. V.: Feasibility of Combining Linear Theory and Impact Methods for the Analysis and Design of High Speed Configurations. NASA CR-3069, 1978.

2. Analysis and Design of Supersonic Wing-Body Combinations, Including Flow Properties in the Near Field. 1967.
   Woodward, F. A.; Tinoco, E. N.; and Larsen, J. W.: Part I - Theory and Application. NASA CR-73106.

   La Rowe, E.; and Love, J. E.: Part II - Digital Computer Program Description. NASA CR-73107.

3. Gentry, A. E.; et al.: The Mark IV Supersonic-Hypersonic Arbitrary-Body Program. AFFDL-TR-73-159, Nov. 1973.

4. Jernell, Lloyd S.: Comparisons of Theoretical and Experimental Pressure Distributions Over a Wing-Body Model at High Supersonic Speeds. NASA TN D-6480, 1971.

5. Woodward, F. A.: An Improved Method for the Aerodynamic Analysis of Wing-Body-Tail Configurations in Subsonic and Supersonic Flow. NASA CR-2228, Parts I and II, 1973.

1. Report No.	2. Government Accession No.	3. Recipient's Catalog No.
NASA CR-3314		

4. Title and Subtitle	5. Report Date
COMBINED LINEAR THEORY/IMPACT THEORY METHOD FOR ANALYSIS AND DESIGN OF HIGH SPEED CONFIGURATIONS	September 1980
	6. Performing Organization Code

7. Author(s)	8. Performing Organization Report No.
D. Brooke and D. V. Vondrasek	
	10. Work Unit No.

9. Performing Organization Name and Address	11. Contract or Grant No.
McDonnell Aircraft Company McDonnell Douglas Corporation P.O. Box 516 St. Louis, MO 63166	NAS1-15535
	13. Type of Report and Period Covered Contractor Report 22 Sept '78 - 22 Dec '79
12. Sponsoring Agency Name and Address National Aeronautics and Space Administration Washington, D.C. 20546	14. Sponsoring Agency Code

15. Supplementary Notes

Langley Technical Monitor: C. L. W. Edwards

Final Report

16. Abstract

A combined linear theory/impact theory method is applied to calculate pressure distributions on a wing-body at Mach 4.63. The combined theory is shown to give improved predictions over either linear theory or impact theory alone. The combined theory is also applied in the inverse design mode to calculate optimum camber slopes at Mach 4.63. Comparisons with optimum camber slopes obtained from unmodified linear theory show large differences. Analysis of the results indicate that the combined theory correctly predicts the effect of thickness on the loading distributions at high Mach numbers, and that finite thickness wings optimized at high Mach numbers using unmodified linear theory will not achieve the minimum drag characteristics for which they are designed.

17. Key Words (Suggested by Author(s))	18. Distribution Statement
Aerodynamic Characteristics Aerodynamic Predictions Camber Slopes, Wing-Body Configuration Pressure Distributions High Speed Configurations	Unclassified - Unlimited Subject Category 02

19. Security Classif (of this report)	20. Security Classif (of this page)	21. No. of Pages	22. Price
Unclassified	Unclassified	31	A03